Jundishapur J Nat Pharm Prod. 2026 May; 21(2): e170836 https://doi.org/10.5812/jjnpp-170836

Published Online: 2026 May 31 **Research Article**

Comparative Pharmacokinetic Analysis of Albendazole Loaded in Solid Lipid Nanoparticles and Microemulsion in Hepatic and Pulmonary Tissues of Experimental Hydatidosis Murine Models

Mahmoud Rahdar [1,2], Abdollah Rafiei [1,2], Mehdi Safdarian [3], Behzad Sharif Makhmalzadeh [3], kereshmeh Fakharzadeh Jahromi [1,2,*]

[1] Infectious and Tropical Diseases Research Center, Health Research Institute, Ahvaz Jundishapur University of Medical Sciences, Ahvaz, Iran
[2] Department of Parasitology, School of Medicine, Ahvaz Jundishapur University of Medical Sciences, Ahvaz, Iran
[3] Nanotechnology Research Center, Medical Basic Sciences Research Institute, Ahvaz Jundishapur University of Medical Sciences, Ahvaz, Iran

[*] ***Corresponding Author:*** Infectious and Tropical Diseases Research Center, Health Research Institute, Ahvaz Jundishapur University of Medical Sciences, Ahvaz, Iran. Email: k_fakharzad@yahoo.com

Received: 25 February, 2026; **Revised:** 22 April, 2026; **Accepted:** 19 May, 2026

Abstract

Background: Pharmacological intervention plays a critical role in managing cystic echinococcosis, both preoperatively and postoperatively, to reduce the risk of recurrence and treat inoperable cases. Therefore, enhancing therapeutic efficacy against hydatid cysts through novel albendazole (ABZ) formulations is essential.

Objectives: This study evaluated the tissue-specific drug absorption profiles of ABZ-loaded solid lipid nanoparticles (ABZ-SLNs) and microemulsions (ABZ-MEs) in a BALB/c mouse model of experimental hydatidosis, with the aim of improving tissue drug uptake through nanoparticle-based delivery systems.

Methods: Twenty-five male BALB/c mice were intraperitoneally inoculated with viable *Echinococcus granulosus* protoscolices isolated from sheep hepatic hydatid cysts. After a 6-month infection establishment period, the animals were stratified into 5 randomized groups (n = 5/group). The study groups received daily oral gavage with albendazole suspension, ABZ-ME, or ABZ-SLN at 20 mg/kg for 30 consecutive days. Subsequently, hepatic and pulmonary tissues were harvested, and the amount of drug extracted from the tissues was measured using high-performance liquid chromatography (HPLC).

Results: Both ABZ-SLN and ABZ-ME had particle sizes < 150 nm, drug loading > 60%, and sustained-release profiles. Tissue ABZ levels were significantly higher with ABZ-SLN and ABZ-ME than with the aqueous suspension ($P < 0.05$), and pulmonary concentrations exceeded hepatic levels for all formulations.

Conclusions: ABZ-SLN and ABZ-ME significantly enhanced ABZ distribution and tissue uptake, which were attributed to their lipid nature and nanoscale particle size. Their sustained-release profiles suggest that these formulations act as drug depots and enhance systemic therapeutic delivery.

Keywords: Hydatid Cyst, Echinococcosis, Albendazole, Solid Nanoparticle, Microemulsion

1. Background

Cystic echinococcosis (CE) is a globally significant zoonotic helminthiasis characterized by diverse clinical manifestations and remains endemic in both developed and developing countries (1-3). The infection is caused by the metacestode stage of *Echinococcus granulosus* and manifests in accidental human hosts through the development of characteristic fluid-filled cysts, predominantly affecting the hepatic (68% - 89%) and pulmonary (10% - 30%) parenchyma (1, 4).

Surgical intervention is the primary treatment option for human CE. Combination therapy involving surgery and albendazole (ABZ) has been shown to reduce the likelihood of disease recurrence (5). When surgical intervention is contraindicated, chemotherapy with benzimidazole derivatives becomes necessary (4).

How to Cite: Rahdar M, Rafiei A, Safdarian M, Sharif Makhmalzadeh B, Fakharzadeh Jahromi K. Comparative Pharmacokinetic Analysis of Albendazole Loaded in Solid Lipid Nanoparticles and Microemulsion in Hepatic and Pulmonary Tissues of Experimental Hydatidosis Murine Models. Jundishapur J Nat Pharm Prod. 2026;21(2):e170836. doi: https://doi.org/10.5812/jjnpp-170836

Despite its therapeutic effects, ABZ administration presents substantial pharmacokinetic challenges, particularly poor aqueous solubility and limited intestinal absorption (6, 7). To address the challenges posed by poorly water-soluble drugs, various strategies have been implemented, including the use of nanoparticles and emulsions. The advantages of nanomedicines include improved bioavailability and stability, versatile routes of administration, controlled drug release, and reduced toxicity (7). In many instances, nanomedicines passively accumulate in infected tissues (8).

Additional advantages of nanocrystals include reduced effective doses and minimized adverse effects (9). Solid lipid nanoparticles (SLNs) and self-emulsifying drug delivery systems (SEEDS) have attracted considerable interest as viable alternatives to traditional colloidal carriers for a range of therapeutic applications (10). Microemulsions facilitate rapid transit through the stomach, thereby enhancing drug dissolution and permeation within the gastrointestinal tract. In vitro studies have demonstrated that the permeability and protoscolicidal activity of ABZ encapsulated in lipid particles are superior to those of free ABZ (10, 11). Emerging preclinical investigations have demonstrated enhanced protoscolicidal activity of biogenic nanoparticle-encapsulated ABZ formulations against *E. granulosus* in murine models (4, 7, 12).

Another disadvantage associated with ABZ is the occurrence of adverse effects during treatment. Documented adverse effects include weight loss, anemia, leukopenia, hypercholesterolemia, and proteinuria (12-14).

2. Objectives

The aim of this study was to evaluate the in vivo efficacy of various ABZ formulations, namely ABZ suspension, ABZ-SLN, and ABZ-ME, against experimental hydatidosis in BALB/c mice. Because hydatid cyst metabolites may interfere with the pharmacokinetic properties of drug absorption, an experimental hydatid infection model was established to approximate the natural pathological conditions of the disease. After 1 month of therapy, ABZ concentrations in hepatic and pulmonary tissues were measured, and the organ distribution of each formulation was compared by HPLC.

3. Methods

3.1. Preparation of Hydatid Cyst Protoscolices

Protoscolices were isolated from hepatic hydatid cysts of sheep at the Ahvaz Central Abattoir and transported to the Department of Parasitology, Faculty of Medicine. The protoscolices were washed 3 times with phosphate-buffered saline (PBS), and viability (> 95%) was confirmed using 0.1% eosin (Merck KGaA, Germany). Viable protoscolices were stored in RPMI medium supplemented with penicillin-streptomycin (BIO-IDEA, Iran) at 4°C and adjusted to a concentration of 4000 protoscolices/mL for subsequent use.

3.2. Experimental Animals and Challenge

The study protocol was approved by the Specialized Ethics Committee for Laboratory Animals under approval code IR.AJUMS.ABHC.REC.1400.061. A total of 25 male BALB/c mice, weighing 18 - 20 g and aged 4 - 8 weeks, were obtained from the Razi Institute Research Center in Hesarak, Karaj, Iran. The mice were divided into 5 groups, and each animal received an intraperitoneal injection of 0.5 mL of a solution containing 2000 protoscolices. The animals were housed in the animal facility of the Faculty of Veterinary Medicine, Shahid Chamran University, under controlled environmental conditions, including a 12-hour light/dark cycle, a temperature range of 22 - 25°C, and 60% relative humidity. Food and water were provided ad libitum for 6 months. All infected mice exhibited viable cysts upon dissection, confirming the adequacy of the infection model.

3.3. Preparation of Albendazole Microemulsion

For the oil base, oleic acid (Samchun, Korea) was combined with Transcutol P (Gattefossé, France) at a ratio of 10:1 (v/v) and thoroughly mixed. The oil phase was then combined with the drug, after which a mixture of surfactants (Tween 80 and Labrasol, 1:1) and a co-surfactant (3:1) was added. Samples exhibiting no turbidity were selected as the appropriate titers.

3.4. Preparation of Albendazole Nanoparticles

Solid lipid nanoparticles were prepared using the cold homogenization method. Briefly, 0.3 g of cholesterol (Solarbio, China), 0.3 g of stearic acid (Applichem, Germany), and 0.1 g of oleic acid (Samchun, Korea) were melted under indirect heating at 65°C. Subsequently, half of the surfactant components, comprising 0.1 g of Tween 80, 0.1 g of Labrasol (Gattefossé, France), and 0.05 g of Capryol (Gattefossé, France), were incorporated into the oily mixture. Then, 0.075 g of albendazole (Sigma, Germany) was added.

Next, 3 mL of the aqueous phase (distilled water) and the remaining half of the surfactant were added to the lipid mixture. The resulting mixture was stirred for 3 minutes using a magnetic stirrer and then sonicated for 32 minutes with a sonicator (Elmasonic, Germany). Finally, 7 mL of cold water (4°C) mixed with polyethylene glycol at a 1:4 ratio was added, and the entire mixture was homogenized for 20 minutes at 12000 rpm using a homogenizer (Heidolph Silent Crusher M, Germany).

3.5. Morphology and Size Characterization

The particle size of both blank SLNs and drug-loaded nanoparticles was assessed using a particle size analyzer (Scatteroscope-qudix, Korea). For scanning electron microscopy (SEM), thin-film samples were prepared, dried at room temperature, and then sent to the Razi Metallurgy Research Center. The acquired images were considered suitable for evaluating morphology and particle size.

3.6. Drug Loading Efficiency

The prepared drug-loaded nanoparticles were centrifuged in a refrigerated microcentrifuge at 25000 rpm for 15 minutes. The 3 aqueous fractions obtained after triple washing with water were pooled, and the drug concentration in the resulting supernatant was measured by HPLC using a C8 column. Drug loading was calculated by subtracting the drug content in the supernatant from the initial drug amount used in the formulation. Loading efficiency was expressed as the percentage of loaded drug relative to the total initial drug amount.

3.7. Drug Release Profile from Drug-Loaded Microemulsion and Solid Lipid Nanoparticles

To evaluate drug release, a static Franz diffusion cell system was used. The concentrations of the released drug were quantified using an HPLC system (Agilent Technologies 1260 Infinity II, USA) equipped with a C8 column. The mobile phase consisted of acetonitrile (Samchun, Korea) and trifluoroacetic acid (Merck, Germany). The concentration of the released drug was determined using a standard curve, and the area under the curve (AUC) was subsequently calculated.

3.8. Treatment of Mice with Drug Formulations

Six months after the initial challenge, all study groups received various formulations of ABZ orally at a dosage of 20 mg/kg/day for 30 days. The groups were as follows:

1) Albendazole suspension (20 mg/kg)

2) Nano-albendazole (20 mg/kg)

3) Albendazole microemulsion (20 mg/kg)

4) Solid lipid nanoparticles containing all nanomedicine components except albendazole

5) Distilled water (control)

Following the treatment period, the animals were euthanized using a ketamine-xylazine combination at a dose of 50 mg/kg. Hepatic and pulmonary tissues were then harvested and stored at -70°C until analysis.

3.9. Drug Extraction from Tissues

Tissue samples were weighed and thoroughly homogenized, after which 1.5 mL of 0.01 M monobasic phosphate buffer (pH 10) was added. Homogenization was performed for 5 - 10 minutes using a homogenizer (Heidolph Silent Crusher M, Germany). Subsequently, 3 mL of an extraction solvent consisting of ethyl acetate and acetonitrile at a 1:5 ratio was added, and the mixture was homogenized for an additional 10 minutes.

The samples were then centrifuged at 5000 rpm for 10 minutes, and the supernatant was collected. An additional 3 mL of the extraction solvent was added to the remaining pellet, followed by homogenization and a second centrifugation. The supernatant from this step was combined with the previously collected supernatant. Next, 8 mL of n-hexane (Merck, Germany) was added to the pooled supernatant, and the mixture was vigorously agitated for 10 minutes before centrifugation at 3500 - 4000 rpm for 10 minutes. The upper n-hexane layer was discarded, and this extraction procedure was repeated once more. The remaining liquid was evaporated under vacuum using a rotary evaporator set at 40°C. The resulting residue was reconstituted in 1 mL of HPLC mobile phase (80% acetonitrile and 20% 0.01% trifluoroacetic acid) and thoroughly vortexed. Drug concentration was measured using the HPLC system under the conditions described previously. Drug concentration in the tissue was determined by plotting a standard curve and performing the necessary calculations.

Extraction recovery was assessed in triplicate by spiking blank tissue homogenates with albendazole (10 μg/g) and processing them identically to the study samples. The mean recovery (± SD, n = 3) was 87.04% ± 3.76% for liver and 90.88% ± 4.21% for lung. All reported tissue concentrations were corrected using these recovery values.

3.10. Statistical Analysis

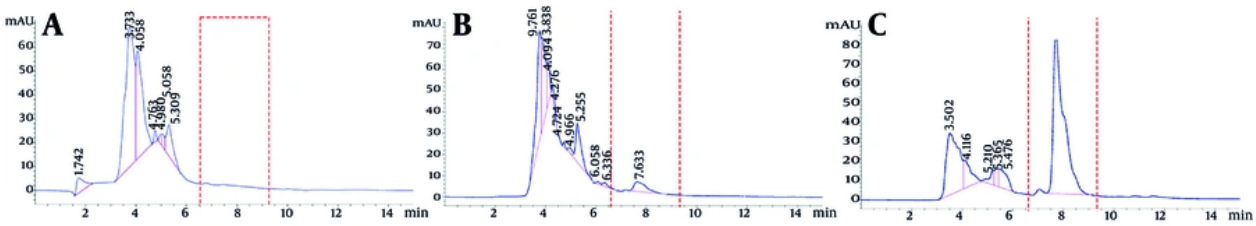

Figure 1. HPLC chromatograms showing: A, tissue extract from the blank SLN control group (Group 4) exhibiting no peak at 7.7 minutes; B, albendazole detected at 7.7 minutes in tissue from SLN-treated mice; and C, the same sample as in (B) spiked with 40 ppm albendazole standard, confirming peak identity. Conditions: C8 column (250 × 4.6 mm, 5 µm); mobile phase: acetonitrile:0.01% trifluoroacetic acid (80:20); flow rate: 1.0 mL/min; detection: 285 nm; injection volume: 20 µL.

All statistical analyses were performed using SPSS software version 21. A significance level of $P < 0.05$ was adopted for all tests. Before parametric analyses, data normality was assessed using the Kolmogorov-Smirnov test. Data conforming to a normal distribution were analyzed using analysis of variance (ANOVA) and Student t-test. For multiple-group comparisons, the Tukey post hoc test was applied. When data deviated from a normal distribution, nonparametric tests, such as the Mann-Whitney U test, were used. A P value < 0.05 was considered statistically significant for all analyses.

4. Results

4.1. HPLC Method Validation

HPLC analysis successfully detected ABZ in tissue samples from SLN-treated mice, with a characteristic peak at a retention time of 7.7 minutes. To confirm method accuracy, samples were spiked with 40 ppm ABZ standard, resulting in a clear increase in peak intensity, while the retention time remained unchanged (Figure 1).

4.2. Repeatability and Accuracy of the HPLC Test

The repeatability and accuracy of the HPLC method for ABZ quantification were evaluated using standard concentrations analyzed under intraday and interday conditions. A standard deviation $< 5\%$ indicated acceptable precision, whereas accuracy $> 94\%$ was considered indicative of good method validity. As shown in Table 1, the repeatability and accuracy of the HPLC method were confirmed.

4.3. Limit of Quantitation

The limit of quantitation (LOQ) represents the minimum quantifiable concentration detectable by the HPLC method; values exceeding this threshold are considered valid and reportable. The LOQ was determined using a calculation incorporating 2 critical parameters: the slope of the calibration curve and the standard deviation of residuals derived from regression analysis. Using this approach, the LOQ was established at 0.17 ppm. All concentration measurements recorded in this investigation exceeded the 0.17-ppm threshold, thereby meeting the validity criterion for the quantitation limit.

4.4. Albendazole Solubility Assay

The solubility of ABZ in the oil, surfactant, co-surfactant, and, finally, in a combination of all solvents was determined using UV spectrophotometry at a wavelength of 285 nm. These results were subsequently used to formulate an ABZ microemulsion. The findings are presented in Table 2.

This investigation systematically evaluated the phase behavior and microemulsion formation characteristics of albendazole-containing systems through pseudoternary phase diagram analysis. Phase diagrams were constructed at 2 distinct surfactant-to-co-surfactant (S:CoS) mass ratios, 1:1 and 3:1, as depicted in Figure 2. The shaded regions within the diagrams demarcate the microemulsion existence zones, and the darkened areas correspond to optically isotropic, thermodynamically stable microemulsion phases.

4.5. Characteristics of Albendazole-Loaded Solid Lipid Nanoparticles

4.5.1. Particle Size

Particle size analysis showed a mean hydrodynamic diameter of 139 ± 10 nm with a narrow size distribution (polydispersity index [PDI] = 0.140). Drug-loaded solid lipid nanoparticles exhibited slightly larger dimensions

Table 1. Repeatability and Accuracy of HPLC for ABZ Quantification

Albendazole Concentration (ppm)	Repeatability, Intraday	Repeatability, Interday	Accuracy, Intraday	Accuracy, Interday
0.5	4.2	3.6	94.8 ± 2.6	96.5 ± 5.2
1.0	3.9	4.7	101.8 ± 5.7	99.3 ± 5.3
10.0	3.8	4.1	109.2 ± 3.2	100.8 ± 4.9
20.0	2.2	3.3	102.7 ± 4.4	99.1 ± 4.4
40.0	3.5	4.6	96.3 ± 6.5	99.9 ± 3.4

Table 2. Albendazole Solubility in Formulation Components (Mean ± SD, N = 3)

Components	Solubility (g/mL)
Transcutol P and oleic acid	8.00 ± 0.38
Labrasol and Tween 80	4.20 ± 0.29
Capryol	1.85 ± 0.19
Transcutol P and oleic acid, Labrasol, Tween 80, and Capryol	13.60 ± 1.95

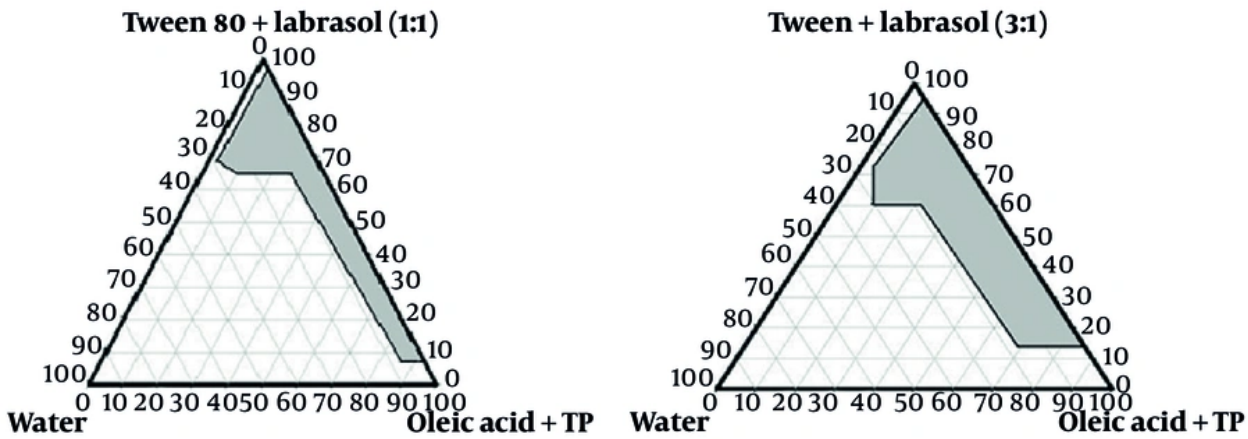

Figure 2. Microemulsion formation characteristics of albendazole-containing systems through pseudoternary phase diagram analysis at 2 distinct surfactant:co-surfactant (S:CoS) mass ratios: 1:1 and 3:1.

(147 ± 12 nm; PDI = 0.160). These findings indicate a suitable particle size range, suggesting that incorporation of ABZ did not substantially alter particle size or PDI. Both formulations exhibited a satisfactory PDI, a pivotal attribute for nanoparticles intended for systemic action (Figure 3).

4.5.2. Albendazole Loading and Release Results

Pharmaceutical characterization showed entrapment efficiencies of 62.7% ± 5.3% for ABZ-ME and 59% for ABZ-SLNs, as illustrated in Figures 4 and 5. The dissolution profile demonstrated sustained release kinetics, characterized by the absence of an initial burst phase. Quantitative analysis showed limited drug release during the early phase, with < 10% cumulative release within the initial 8-hour period. Progressive release kinetics were maintained through 72 hours, achieving approximately 50% total drug release.

4.6. Drug Concentration in Tissues

Table 3 presents drug concentrations in pulmonary and hepatic tissues relative to the total administered

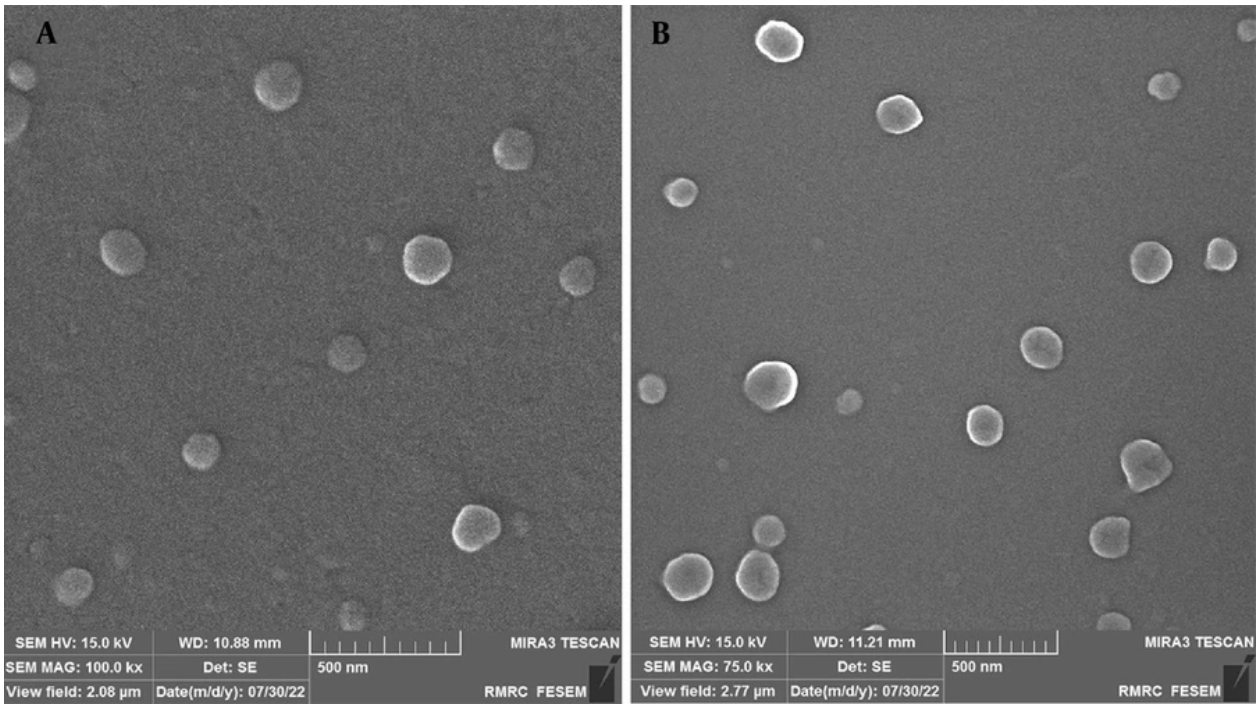

Figure 3. Representative SEM images of A, blank SLNs (145.5 ± 12.8 nm) and B, ABZ-SLNs (162.8 ± 13.5 nm).

dose of conventional ABZ, ABZ-ME, and ABZ-SLN over 1 month. All formulations were administered orally to the study groups for 1 month, 6 months after intraperitoneal challenge with 2000 protoscolices.

Statistical analysis indicated that ABZ-ME and ABZ-SLN showed significantly higher drug concentrations in both pulmonary and hepatic tissues than conventional ABZ ($P < 0.05$). In the conventional ABZ group, no significant difference was observed between pulmonary and hepatic tissue drug levels ($P > 0.05$). Similarly, in the ABZ-ME group, there was no significant difference between pulmonary and hepatic tissue drug levels ($P > 0.05$). Likewise, no significant difference was found between pulmonary and hepatic ABZ levels in the ABZ-SLN group ($P > 0.05$).

5. Discussion

ABZ, a broad-spectrum benzimidazole anthelmintic, is widely used in human and veterinary medicine for the treatment of nematode infestations and larval-stage cestode infections.

Current clinical use shows distinct pharmacological profiles depending on the indication. For gastrointestinal nematode infections, a regimen of 400 mg/day for 2 days has an excellent safety profile. However, treatment of larval-stage cestode infections requires prolonged high-dose therapy (800 mg/day for 3 - 6 months) to achieve therapeutic concentrations.

Following oral administration, ABZ reaches peak plasma concentration (Cmax) within 2 - 3 hours. Hepatic microsomal enzymes rapidly metabolize ABZ into its pharmacologically active sulfoxide derivative (ABZ-SO) and inactive sulfone metabolite (ABZ-SN), facilitating renal excretion through enhanced aqueous solubility (15). The maximum plasma concentration (Cmax) of ABZ sulfoxide reaches 0.16 µg/mL, and the elimination half-life (t1/2) ranges from 8 to 12 hours (16). ABZ bioavailability can be enhanced by several factors, including a fatty diet, body weight, sex, age, and concurrent infectious diseases (17). Administration of ABZ with fatty foods or grapefruit juice can increase bioavailability by up to 6.5- and 3.2-fold, respectively, which is particularly important for the treatment of tissue parasites (15). This phenomenon may be attributed to increased drug solubility (18). Whittaker et al. reported that ABZ sulfoxide bioavailability and ABZ half-life vary by age, with significant differences

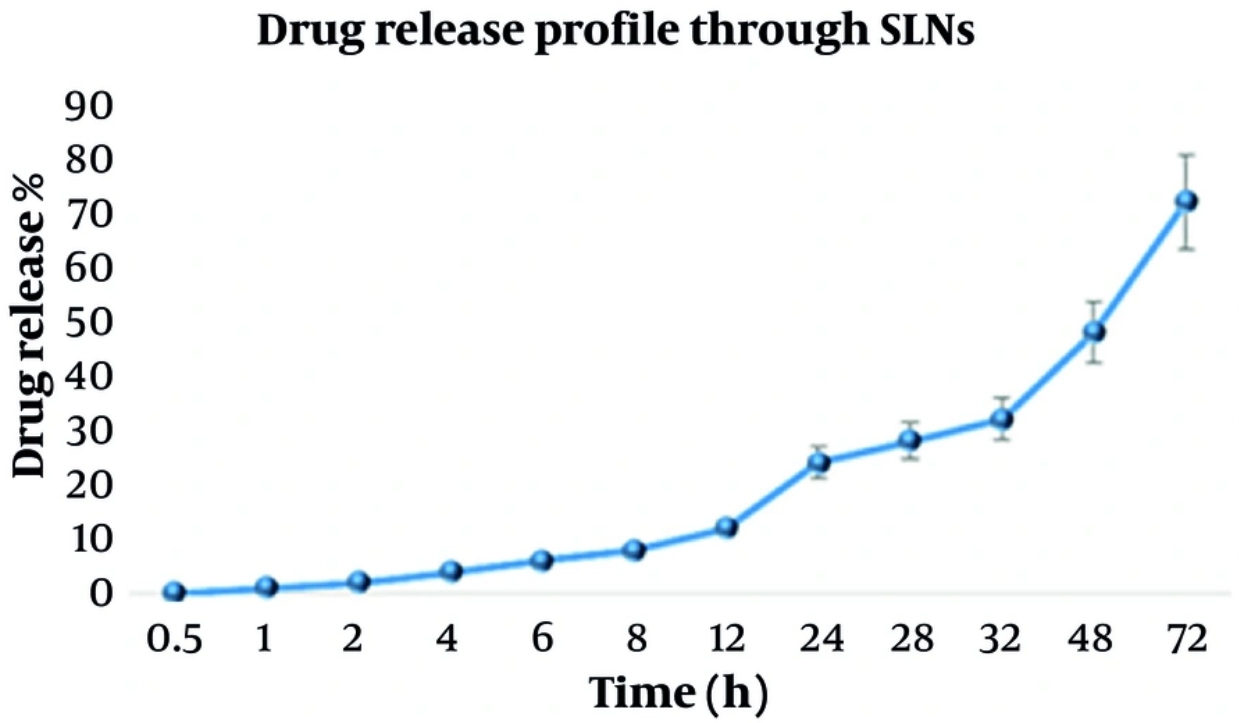

Figure 4. In vitro release profile of ABZ from solid lipid nanoparticles (SLNs), demonstrating sustained release kinetics over 72 hours (n = 3).

between adults and children (17). Capece et al. demonstrated significant sex-related differences in Tmax and Cmax plasma drug levels between male and female goats. Following administration of 10 mg/kg ABZ, male goats exhibited a Tmax of 18.33 hours and a Cmax of 4.4 μg/mL for ABZ sulfoxide, whereas female goats showed a Tmax of 16.67 hours and a Cmax of 3 μg/mL (19).

In the present study, 3 ABZ formulations, ABZ suspension, ABZ-ME, and ABZ-SLN, were evaluated in hepatic and pulmonary tissues of BALB/c mice. The findings showed that ABZ levels in the ABZ-ME and ABZ-SLN groups were significantly higher than those in the hepatic and pulmonary tissues of the ABZ suspension group ($P < 0.05$). In the ABZ suspension group, drug concentrations were 0.0042 mg/g in hepatic tissue and 0.0051 mg/g in pulmonary tissue. In contrast, the ABZ-ME group showed concentrations of 0.7100 mg/g in hepatic tissue and 1.2200 mg/g in pulmonary tissue. Similarly, the ABZ-SLN group exhibited concentrations of 0.4360 mg/g in hepatic tissue and 0.6600 mg/g in pulmonary tissue. These results indicate that advanced ABZ formulations are more effective for the treatment of tissue hydatidosis.

Although ABZ measurement in plasma has been reported in several studies, most articles quantify ABZ metabolites rather than the parent compound because of rapid hepatic metabolism in patients (20). Arroyo et al. reported that ABZ-SO levels in 118 patients with neurocysticercosis receiving 22 mg/kg ABZ for 10 days ranged from 194 to 1364.6 ng/mL in plasma, with variations correlating with age and sex (21).

Permana et al. observed that the concentration gradient across tissues followed the order hepatic > kidney > spleen (22).

In the present study, higher drug concentrations were observed in lung tissue than in liver tissue. This finding may be attributable to hepatic clearance and enterohepatic recirculation, which could reduce measured levels of the parent drug in the liver at a single terminal time point, whereas the lung may act as a slower-release compartment. However, in the absence

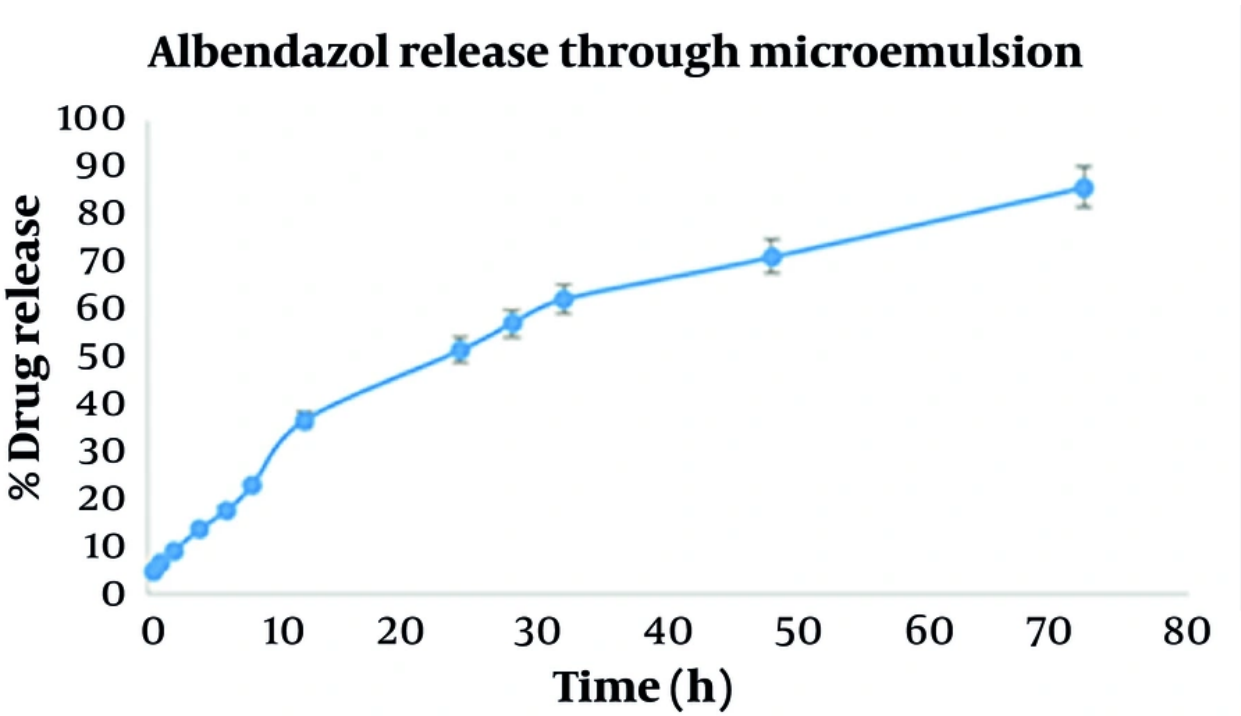

Figure 5. Comparative release kinetics of the albendazole microemulsion formulation (ABZ-ME), showing a rapid initial release phase followed by sustained drug release (n = 3).

of plasma pharmacokinetic (PK) data, this interpretation remains hypothetical.

These findings confirm hepatic accumulation of ABZ metabolites and align with our results; however, discrepancies in absolute concentrations may reflect differences in detection methods, treatment duration, and formulation strategies.

In the current study, the concentration of ABZ in the ABZ-ME and ABZ-SLN groups was significantly higher than that in the ABZ suspension group ($P < 0.05$). Fabbri et al. additionally reported a 183% increase in ABZ bioavailability in the brain tissue of rats with experimental cysticercosis treated with ABZ-loaded lipid nanocapsules compared with the ABZ suspension group, with a 2-fold enhancement in therapeutic efficacy (23). Consistent with these findings, the concentration of ABZ in pulmonary tissue exceeded that in hepatic tissue across the ABZ-ME and ABZ-SLN groups ($P < 0.05$). Notably, ABZ-SLN demonstrated greater drug accumulation in both hepatic and pulmonary tissues compared with ABZ-ME ($P < 0.05$), suggesting superiority for systemic tissue distribution. These results align with studies on ABZ-lipid nanocapsules in murine models of cystic echinococcosis, in which enhanced plasma and tissue ABZ levels correlated with improved clinical outcomes (24, 25). In addition, Mukherjee et al. demonstrated that a supersaturated SEEDS for ABZ achieved a 52% higher Cmax ($P = 0.019$) and 56% greater AUC over 24 hours than the standard ABZ suspension (26).

Due to certain experimental limitations, a blank microemulsion group was not included in the current study. However, including a blank microemulsion control in future investigations would provide deeper insight into the inherent effects of the carrier system.

5.1. Conclusions

The present study demonstrates that both ABZ-SLN and ABZ-ME significantly enhance tissue drug distribution compared with conventional ABZ suspension, with pulmonary concentrations consistently exceeding hepatic levels across all formulations. The observed pharmacokinetic improvements, including sustained release profiles and greater tissue accumulation, support these nanocarriers as promising delivery systems that warrant further

Table 3. Albendazole Concentration in Tissues After 1 Month of Treatment [a]

Formulation Type	Drug Recovered		Percentage of Drug Recovered	
	Hepatic Tissue (mg/g Tissue)	Pulmonary Tissue (mg/g Tissue)	Hepatic Tissue	Pulmonary Tissue
ABZ	0.0042 ± 0.0010	0.0051 ± 0.0014	0.72 ± 0.11	0.78 ± 0.17
ABZ-ME	0.7100 ± 0.1200	1.2200 ± 0.1600	2.25 ± 0.47	3.14 ± 0.51
ABZ-SLN	0.4360 ± 0.0700	0.6600 ± 0.1100	4.45 ± 0.82	4.21 ± 0.12

[a] Abbreviation: ABZ, albendazole.

investigation in therapeutic models. However, 2 key limitations warrant consideration: 1) the absence of metabolite profiling, particularly active ABZ-SO and inactive ABZ-SN levels; and 2) unmeasured drug concentrations in cyst fluid. These findings indicate that ABZ-SLN and ABZ-ME markedly enhance tissue delivery of the parent drug; however, translation to clinical efficacy requires demonstration of elevated active metabolite levels. These gaps highlight critical directions for future research to fully characterize the therapeutic potential of these advanced formulations.

Acknowledgements

This research was extracted from the PhD thesis of Kereshmeh Fakharzadeh Jahromi and was financially supported by the Infectious and Tropical Diseases Research Center, Health Research Institute, Ahvaz Jundishapur University of Medical Sciences, Ahvaz, Iran (Grant No. OG-0044). The authors also sincerely thank Yalda Nazari Khoraskani and Nasim Hasanvand for their valuable assistance in conducting the laboratory experiments.

Footnotes

AI Use Disclosure: The authors declare that no generative AI tools were used in the creation of this article.

Authors' Contribution: Study concept/design: A. R. and B. S. H.; Data analysis/interpretation: B. S. H., M. S., and M. R.; Manuscript drafting: M. R. and K. F.; Critical revision: M. R., A. R., M. S., B. S. H.; Statistical analysis: M. R., B. S. H., and M. S.; Laboratory experiments: K. F., M. R., and M. S.; All authors reviewed and approved the final manuscript.

Conflict of Interests Statement: The authors declare no competing interests.

Data Availability: The dataset presented in the study is available on request from the corresponding author during submission or after publication.

Ethical Approval: This study was approved by the Animal Ethics Committee of Jundishapur University of Medical Sciences, under ethics code number IR.AJUMS.ABHC.REC.1400.061.

Funding/Support: This research is financially supported by Infectious and Tropical Diseases Research Center, Health Research Institute, Ahvaz Jundishapur University of Medical Sciences, Ahvaz, Iran as grant number OG-0044 and ethical number IR.AJUMS.ABHC.REC.1400.061.

References

1. Rahimi MT, Ahmadpour E, Rahimi Esboei B, Spotin A, Kohansal Koshki MH, Alizadeh A, et al. Scolicidal activity of biosynthesized silver nanoparticles against Echinococcus granulosus protoscolices. *Int J Surg*. 2015;**19**:128-33. [PubMed ID: 26028438]. https://doi.org/10.1016/j.ijsu.2015.05.043.
2. Beigh AB, Darzi MM, Bashir S, kashani B, Shah A, Shah SA. Gross and histopathological alterations associated with cystic echinococcosis in small ruminants. *J Parasit Dis*. 2017;**41**(4):1028-33. [PubMed ID: 29114137]. [PubMed Central ID: PMC5660029]. https://doi.org/10.1007/s12639-017-0929-z.
3. Fakharzadeh Jahromi K, Rafiei A, Rahdar M, Bahreini A. Evaluation of the Protoscolicidal Effectiveness of Hypertonic Saline, Silver Nitrate, Ethanol, Using Sponge Pad Method and Injecting into Fertile Hydatid Cysts. *Iran J Parasitol*. 2022;**17**(2):223-30. [PubMed ID: 36032753]. [PubMed Central ID: PMC9363256]. https://doi.org/10.18502/ijpa.v17i2.9540.
4. Marzban A, Cheraghipour K, Rouzbahani AK, Fallahi S, Taherpour F, Moradifard F, et al. Recent Advances in Therapeutic Strategies against Hydatid Cysts using Nanomaterials: A Systematic Review. *Letters in Drug Design & Discovery*. 2023;**20**(9):1185-93. https://doi.org/10.2174/1570180819666220922104034.
5. Gomez IGC, López-Andújar R, Belda Ibáñez T, Ramia Ángel JM, Moya Herraiz Á, Orbis Castellanos F, et al. Review of the treatment of liver hydatid cysts. *World J Gastroenterol*. 2015;**21**(1):124-31. [PubMed ID: 25574085]. [PubMed Central ID: PMC4284328]. https://doi.org/10.3748/wjg.v21.i1.124.
6. Paredes AJ, Bruni SS, Allemandi D, Lanusse C, Palma SD. Albendazole nanocrystals with improved pharmacokinetic performance in mice. *Therapeutic delivery*. 2018;**9**(2):89-97. [PubMed ID: 29325510]. https://doi.org/10.4155/tde-2017-0090.

7. Shnawa BH. Advances in the Use of Nanoparticles as Anti-Cystic Echinococcosis Agents: A Review Article. *Journal of Pharmaceutical Research International*. 2018;**24**(1):1-14. https://doi.org/10.9734/JPRI/2018/44642.
8. Ventola CL. Progress in Nanomedicine: Approved and Investigational Nanodrugs. *P & T: a peer-reviewed journal for formulary management*. 2017;**42**(12):742-55. [PubMed ID: 29234213]. [PubMed Central ID: PMC5720487].
9. Fülöp V, Jakab G, Bozó T, Tóth B, Endrésik D, Balogh E, et al. Study on the dissolution improvement of albendazole using reconstitutable dry nanosuspension formulation. *European journal of pharmaceutical sciences: official journal of the European Federation for Pharmaceutical Sciences*. 2018;**123**:70-8. [PubMed ID: 30010031]. https://doi.org/10.1016/j.ejps.2018.07.027.
10. Aminpour S, Rafiei A, Jelowdar A, Kouchak M. Evaluation of the Protoscolicidal Effects of Albendazole and Albendazole Loaded Solid Lipid Nanoparticles. *Iranian journal of parasitology*. 2019;**14**(1):127-35. [PubMed ID: 31123477]. [PubMed Central ID: PMC6511589]. https://doi.org/10.18502/ijpa.v14i1.726.
11. Jelowdar A, Rafiei A, Abbaspour MR, Rashidi I, Rahdar M. Efficacy of combined albendazol and praziquntel and their loaded solid lipid nanoparticles components in chemoprophylaxis of experimental hydatidosis. *Asian Pacific journal of tropical biomedicine*. 2017;**7**(6):549-54. https://doi.org/10.1016/j.apjtb.2017.05.011.
12. Pion SDS, Chesnais CB, Bopda J, Louya F, Fischer PU, Majewski AC, et al. The impact of two semiannual treatments with albendazole alone on lymphatic filariasis and soil-transmitted helminth infections: a community-based study in the Republic of Congo. *Am J Trop Med Hyg*. 2015;**92**(5):959-66. [PubMed ID: 25758650]. [PubMed Central ID: PMC4426585]. https://doi.org/10.4269/ajtmh.14-0661.
13. Moser W, Coulibaly JT, Ali SM, Ame SM, Amour AK, Yapi RB, et al. Efficacy and safety of tribendimidine, tribendimidine plus ivermectin, tribendimidine plus oxantel pamoate, and albendazole plus oxantel pamoate against hookworm and concomitant soil-transmitted helminth infections in Tanzania and Côte d'Ivoire: a randomised, controlled, single-blinded, non-inferiority trial. *Lancet Infect Dis*. 2017;**17**(11):1162-71. [PubMed ID: 28864027]. https://doi.org/10.1016/S1473-3099(17)30487-5.
14. Dayan AD. Albendazole, mebendazole and praziquantel. Review of non-clinical toxicity and pharmacokinetics. *Acta Trop*. 2003;**86**(2 - 3):141-59. [PubMed ID: 12745134]. https://doi.org/10.1016/S0001-706X(03)00031-7.
15. Nagy J, Schipper HG, Koopmans RP, Butter JJ, Van Boxtel CJ, Kager PA. Effect of grapefruit juice or cimetidine coadministration on albendazole bioavailability. *Am J Trop Med Hyg*. 2002;**66**(3):260-3. [PubMed ID: 12139218]. https://doi.org/10.4269/ajtmh.2002.66.260.
16. Hong ST. Albendazole and Praziquantel: Review and Safety Monitoring in Korea. *Infect Chemother*. 2018;**50**(1):1-10. [PubMed ID: 29637747]. [PubMed Central ID: PMC5895825]. https://doi.org/10.3947/ic.2018.50.1.1.
17. Whittaker C, Chesnais CB, Pion SDS, Kamgno J, Walker M, Basáñez MG, et al. Factors associated with variation in single-dose albendazole pharmacokinetics: A systematic review and modelling analysis. *PLoS Negl Trop Dis*. 2022;**16**(10). e0010497. [PubMed ID: 36306320]. [PubMed Central ID: PMC9662735]. https://doi.org/10.1371/journal.pntd.0010497.
18. Jung H, Medina L, García L, Fuentes I, Moreno-Esparza R. Absorption studies of albendazole and some physicochemical properties of the drug and its metabolite albendazole sulphoxide. *J Pharm Pharmacol*. 1998;**50**(1):43-8. [PubMed ID: 9504433]. https://doi.org/10.1111/j.2042-7158.1998.tb03303.x.
19. Capece BPS, Afonso SMS, Lazáro R, Harun M, Godoy C, Castells G, et al. Effect of age and gender in the pharmacokinetics of albendazole and albendazole sulphoxide enantiomers in goats. *Res Vet Sci*. 2009;**86**(3):498-502. [PubMed ID: 18805559]. https://doi.org/10.1016/j.rvsc.2008.08.002.
20. Mirfazaelian A, Dadashzadeh S, Rouini MR. A high performance liquid chromatography method for simultaneous determination of albendazole metabolites in human serum. *J Pharm Biomed Anal*. 2002;**30**(4):1249-54. [PubMed ID: 12408915]. https://doi.org/10.1016/S0731-7085(02)00482-X.
21. Arroyo G, Bustos JA, Lescano AG, Gonzales I, Saavedra H, Rodriguez S, et al. Albendazole Sulfoxide Plasma Levels and Efficacy of Antiparasitic Treatment in Patients With Parenchymal Neurocysticercosis. *Clin Infect Dis*. 2019;**69**(11):1996-2002. [PubMed ID: 30715265]. [PubMed Central ID: PMC6853673]. https://doi.org/10.1093/cid/ciz085.
22. Permana AD, Tekko IA, McCarthy HO, Donnelly RF. New HPLC-MS method for rapid and simultaneous quantification of doxycycline, diethylcarbamazine and albendazole metabolites in rat plasma and organs after concomitant oral administration. *J Pharm Biomed Anal*. 2019;**170**:243-53. [PubMed ID: 30947125]. https://doi.org/10.1016/j.jpba.2019.03.047.
23. Fabbri J, Espinosa JP, Pensel PE, Medici SK, Gamboa GU, Benoit JP, et al. Do albendazole-loaded lipid nanocapsules enhance the bioavailability of albendazole in the brain of healthy mice? Acta tropica. *Acta Tropica*. 2020;**201**. 105215. [PubMed ID: 31600525]. https://doi.org/10.1016/j.actatropica.2019.105215.
24. Pensel PE, Castro S, Allemandi D, Bruni SS, Palma SD, Elissondo MC. Enhanced chemoprophylactic and clinical efficacy of albendazole formulated as solid dispersions in experimental cystic echinococcosis. *Veterinary Parasitology*. 2014;**203**(1):80-6. [PubMed ID: 24572043]. https://doi.org/10.1016/j.vetpar.2014.01.027.
25. Ullio Gamboa GV, Pensel PE, Elissondo MC, Sanchez Bruni SF, Benoit JP, Palma SD, et al. Albendazole-lipid nanocapsules: Optimization, characterization and chemoprophylactic efficacy in mice infected with Echinococcus granulosus. *Exp Parasitol*. 2019;**198**:79-86. [PubMed ID: 30769018]. https://doi.org/10.1016/j.exppara.2019.02.002.
26. Mukherjee T, Plakogiannis FM. Development and oral bioavailability assessment of a supersaturated self-microemulsifying drug delivery system (SMEDDS) of albendazole. *J Pharm Pharmacol*. 2010;**62**(9):1112-20. [PubMed ID: 20796189]. https://doi.org/10.1111/j.2042-7158.2010.01149.x.